7
The production of polarized $e^{\pm}$

Quite dramatic progress has been made in the production and utilization of polarized $e^{\pm}$ beams at CERN's LEP, at HERA at DESY and at the Stanford linear collider SLC. The motivation for trying to overcome the tremendous technical problems involved derives from two sources:

(i) the realization that longitudinally polarized electrons permit extremely accurate measurement of the fundamental parameters of the Standard Model of electroweak interactions;
(ii) the discovery in 1987, by the European Muon Collaboration (Ashman *et al.*, 1988), that only a very small fraction of the proton's spin appeared to be carried by its quarks, leading to what was characterized as a 'crisis in the parton model' (Leader and Anselmino, 1988). This made it important to carry out further studies of deep inelastic lepton–hadron scattering using longitudinally polarized leptons colliding with a longitudinally polarized proton target.

Though not a primary impetus, it turns out also that polarized $e^{\pm}$ permit an exceedingly accurate calibration of the beam energy at LEP and HERA.

The problems involved in having stable polarized beams are quite different in circular storage rings and in linear accelerators. Hence we shall discuss the two cases separately.

7.1 The natural polarization of electrons circulating in a perfect storage ring

As mentioned in the introduction to Chapter 6, in principle a circulating electron beam gradually acquires a natural polarization in which its magnetic moment $\boldsymbol{\mu}_e$ becomes aligned parallel to the guide field **B**. Ultimately

https://doi.org/10.1017/9781009402040.007 Published online by Cambridge University Press

a maximum degree of polarization

$$\mathscr{P}_0 = \frac{8}{5\sqrt{3}} \approx 92\% \tag{7.1.1}$$

is attained (Sokolov and Ternov, 1963). This is known as the Sokolov–Ternov effect. For electrons, with $\boldsymbol{\mu}_e$ opposite in direction to $\mathbf{s}$, the mean spin vector will be polarized antiparallel to $\mathbf{B}$.

We consider an idealized perfectly circular ring of radius R with a uniform guide field $B_0\mathbf{e}_z$ and with all particles having a fixed energy E. Our discussion relies heavily on a very illuminating treatment by Jackson (1976).

At first sight the closeness of $\mathscr{P}_0$ to 100% together with the fact that $\boldsymbol{\mu}_e$ lines up along $\mathbf{B}$ suggests that the phenomenon is trivial, namely that radiative transitions cause the system to populate the state of lowest energy in the hamiltonian $H = -\boldsymbol{\mu} \cdot \mathbf{B}$. This would be true for an isolated spin system, but to regard an electron in a storage ring as an isolated spin system is self-contradictory. This can be seen as follows.

In this picture, in its canonical rest frame the electron would see a magnetic field $\gamma B_0\mathbf{e}_z$, so that the energy levels, in this frame, would have separation

$$\Delta\mathring{E}_{\text{spin}} = \frac{g}{2}\left(\frac{e\hbar\gamma B_0}{mc}\right). \tag{7.1.2}$$

This separation, in the Lab, is

$$\Delta E_{\text{spin}} = \gamma\Delta\mathring{E}_{\text{spin}} = \left(\frac{g\gamma^3}{2}\right)\hbar\Omega_{\text{c}}, \tag{7.1.3}$$

where, for an electron,

$$\Omega_{\text{c}} = \frac{eB_0}{\gamma mc}. \tag{7.1.4}$$

Now consider the orbital angular momentum (kinetic, not canonical) of the electron: it is

$$l\hbar \approx Rp = mR\gamma v$$

so that

$$l = \frac{cmR\gamma\beta}{\hbar} = \left(\frac{R}{\lambda\!\!\!^{-}_e}\right)\gamma\beta \tag{7.1.5}$$

where $\lambda\!\!\!^{-}_e$, the Compton wavelength of the electron, $\approx 4 \times 10^{-13}$ m. For an ultra-relativistic electron with, say, $R \approx 1000$ m, $\gamma \approx 10^5$ and $\beta \approx 1$ we have

$$l \approx 4 \times 10^{21}. \tag{7.1.6}$$

https://doi.org/10.1017/9781009402040.007 Published online by Cambridge University Press

The orbital levels with different values of l_z will be separated by

$$\Delta E_{\text{orbital}} = \hbar\Omega_c. \tag{7.1.7}$$

Thus

$$\frac{\Delta E_{\text{orbital}}}{\Delta E_{\text{spin}}} = \frac{2}{g\gamma^3} \ll 1. \tag{7.1.8}$$

Hence any radiative transition involving energies of order ΔE_{spin} will involve huge changes in l_z and there will exist a strong coupling between the spin and orbital degrees of freedom. In other words the spin system is not at all isolated!

Incidentally, this does not imply that the motion is non-classical, because for an emitted photon whose energy is given by (7.1.3) the electron recoil will imply a change in momentum, using (6.3.29),

$$\Delta p \simeq \frac{g}{2}\left(\frac{\gamma^3\hbar\Omega_c}{c}\right) \simeq \frac{g\gamma^3}{2R}.$$

This yields a large change in l of order

$$\delta l \approx \frac{g}{2}\gamma^3 \approx \frac{g}{2} \times 10^{15}. \tag{7.1.9}$$

Nonetheless,

$$\frac{\delta l}{l} \simeq \frac{g}{2}\left(\frac{\lambda\!\!\!^{-}_e}{R}\right)\gamma^2 \approx 10^{-6} \tag{7.1.10}$$

and so remains very small for our example.

We shall now outline how the effect can be understood in the framework of quasi-classical radiation theory, on the basis of the relativistic motion of the spin vector.

Recall that, in the usual quasi-classical radiation theory, the spontaneous emission of a photon with momentum $\mathbf{k}$ and polarization vector $\boldsymbol{\varepsilon}$ arises from a time-dependent perturbation engendered by the coupling of the charge of the particle to a classical electromagnetic vector potential $\mathbf{A}'(\mathbf{r}, t)$. This is chosen to correspond, in intensity, to having one photon present. Thus one takes

$$H'_{\text{charge}} = -\frac{q}{mc}\mathbf{p}\cdot\mathbf{A}' \tag{7.1.11}$$

with

$$\mathbf{A}' = c\sqrt{\frac{2\pi\hbar}{\omega}}\boldsymbol{\varepsilon}^* e^{i(\omega t - \mathbf{k}\cdot\mathbf{r})}. \tag{7.1.12}$$

https://doi.org/10.1017/9781009402040.007 Published online by Cambridge University Press

To obtain the radiative transitions due to the spin we note that the effective hamiltonian giving rise to the spin motion (6.3.22) is

$$H_{\text{spin}} = -\frac{q}{mc}\mathbf{s}\cdot\left[\left(\frac{g}{2}-1+\frac{1}{\gamma}\right)\mathbf{B}-\left(\frac{g}{2}-1\right)\frac{\gamma}{\gamma+1}(\boldsymbol{\beta}\cdot\mathbf{B})\boldsymbol{\beta}\right.$$
$$\left.-\left(\frac{g}{2}-1+\frac{1}{\gamma+1}\right)\boldsymbol{\beta}\times\mathbf{E}\right] \tag{7.1.13}$$

and we produce a spontaneous transition by taking the electric and magnetic fields to correspond to $\mathbf{A}'$ in (7.1.12), i.e.

$$\begin{aligned}\mathbf{E}' &= -i\sqrt{2\pi\hbar\omega}\,\boldsymbol{\varepsilon}^* e^{i(\omega t-\mathbf{k}\cdot\mathbf{r})} \equiv \mathscr{E}\boldsymbol{\varepsilon}^*\\ \mathbf{B}' &= -i\sqrt{2\pi\hbar\omega}(\hat{\mathbf{k}}\times\boldsymbol{\varepsilon}^*)e^{i(\omega t-\mathbf{k}\cdot\mathbf{r})} = \mathscr{E}(\hat{\mathbf{k}}\times\boldsymbol{\varepsilon}^*).\end{aligned} \tag{7.1.14}$$

We shall simplify life by dealing only with electrons from now on, and so take $g/2-1=0$. Thus the perturbing hamiltonian becomes

$$H'_{\text{spin}} = \frac{e}{\gamma mc}\mathbf{s}\cdot\left(\mathbf{B}'-\frac{\gamma}{\gamma+1}\boldsymbol{\beta}\times\mathbf{E}'\right). \tag{7.1.15}$$

The total hamiltonian is then

$$H = H^0 + H'_{\text{charge}} + H'_{\text{spin}} \equiv H^0 + H' \tag{7.1.16}$$

where H^0 includes the interaction with the guide field $\mathbf{B}_0 = B_0\mathbf{e}_z$, which can be taken to come from a vector potential

$$\mathbf{A}_0 = -\tfrac{1}{2}\mathbf{r}\times\mathbf{B}_0. \tag{7.1.17}$$

Thus, using (7.1.13),

$$\begin{aligned}H^0 &= \sqrt{(c\mathbf{P}^2+e\mathbf{A}_0)^2+m^2c^2}+\frac{1}{\gamma}\frac{e}{mc}\mathbf{s}\cdot\mathbf{B}_0\\ &\equiv H^0_{\text{charge}}+H^0_{\text{spin}}\end{aligned} \tag{7.1.18}$$

where $\mathbf{P}$ is the *canonical* momentum.

The problem is solved hierarchically as follows.

(1) The usual classical motion is obtained from H^0_{charge}, ignoring the influence of the spin upon the orbit (s is explicitly of order $\hbar$).
(2) The unperturbed motion of the spin is then controlled by H^0_{spin}. The influence of the orbital motion has been taken into account in going from (7.1.13) to (7.1.18) (the appearance of $g/2-1+1/\gamma = 1/\gamma$ instead of $g/2$). Because $g=2$ the mean spin vector $\mathbf{s}(t)$ rotates about $\mathbf{B}_0$ at the same angular frequency as $\boldsymbol{\beta}(t)$ (see eqn (6.3.24)), i.e. with the

https://doi.org/10.1017/9781009402040.007 Published online by Cambridge University Press

relativistic cyclotron frequency

$$\omega_c \equiv \Omega_c^{\text{electron}} = \frac{eB_0}{\gamma mc}. \tag{7.1.19}$$

(3) Time-dependent perturbation theory tells us that the probability for the spontaneous emission of a photon with $\mathbf{k}$ in $d^3\mathbf{k}$ $(= \omega^2 d\omega d\Omega/c^3)$ during the time interval $t_1 \to t_2$ is

$$dp = \left| \frac{1}{i\hbar} \int_{t_1}^{t_2} \langle f|H'(t)|i\rangle dt \right|^2 \frac{\omega^2 d\omega d\Omega}{(2\pi c)^3}. \tag{7.1.20}$$

The term H'_{charge} in (7.1.11) gives rise to the usual synchrotron radiation and is of no interest to us here. We thus utilize (7.1.15) for H', in which $\mathbf{s}$ is now the unperturbed spin operator.

It is simplest to work in the Heisenberg picture because there the time-dependent operators obey equations of motion that are formally the same as those governing the motion of the mean values of the operators. Thus, in (7.1.15)

$$\mathbf{s} \to \hat{\mathbf{s}}(t) \equiv (\hbar/2)\,\boldsymbol{\sigma}(t) \tag{7.1.21}$$

where $\boldsymbol{\sigma}(t)$ rotates about $\mathbf{B}_0$ at angular freqency ω_c. Thus, we can take

$$\begin{aligned} \sigma_x(t) &= \sigma_x \cos\omega_c t - \sigma_y \sin\omega_c t \\ \sigma_y(t) &= \sigma_x \sin\omega_c t + \sigma_y \cos\omega_c t \\ \sigma_z(t) &= \sigma_z. \end{aligned} \tag{7.1.22}$$

The perturbation H'_{spin} will give rise to both non-flip and spin-flip emission. Here we are only interested in the latter: if we quantize our states along OZ then spin-flip can only arise from the matrices $\sigma_x(t)$, $\sigma_y(t)$ or, more precisely, from

$$\sigma_\pm(t) = \tfrac{1}{2}\left[\sigma_x(t) \pm i\sigma_y(t)\right] = \sigma_\pm e^{\pm i\omega_c t} \tag{7.1.23}$$

where $\sigma_\pm = (\sigma_x \pm \sigma_y)/2$ are the usual spin-raising and spin-lowering matrices.

Using the fact that for any two vectors $\mathbf{C}$, $\mathbf{D}$,

$$\mathbf{C}\cdot\mathbf{D} = 2(C_+D_- + C_-D_+) + C_zD_z$$

we see that the relevant, spin-flip, part of (7.1.15), is

$$\frac{e\hbar}{\gamma mc}\left[\sigma_+(t)\left(\mathbf{B}' - \frac{\gamma}{\gamma+1}\boldsymbol{\beta}\times\mathbf{E}\right)_- + \sigma_-(t)\left(\mathbf{B}' - \frac{\gamma}{\gamma+1}\boldsymbol{\beta}\times\mathbf{E}\right)_+\right]. \tag{7.1.24}$$

Now, it is known that the radiation from a relativistic particle whose acceleration is perpendicular to its velocity is confined to a narrow cone

https://doi.org/10.1017/9781009402040.007 Published online by Cambridge University Press

about $\mathbf{v}$ of opening angle $\theta \approx 1/\gamma$. So we may, for simplicity, consider a linearly polarized photon with $\mathbf{k}$ in the XY-plane, say along OY. Then we can put

$$\boldsymbol{\varepsilon}^* = (\sin\alpha, 0, \cos\alpha) = (\epsilon_x, 0, \epsilon_z) \tag{7.1.25}$$

and take

$$\boldsymbol{\beta}(t) = \beta(-\sin\omega_c t, \cos\omega_c t, 0). \tag{7.1.26}$$

Then (7.1.24) involves, from (7.1.14),

$$\begin{aligned}\left(\mathbf{B}' - \frac{\gamma}{\gamma+1}\boldsymbol{\beta}\times\mathbf{E}'\right) &= \mathscr{E}\left[(\hat{\mathbf{k}}\times\boldsymbol{\varepsilon}^*) - \frac{\gamma}{\gamma+1}\boldsymbol{\beta}\times\boldsymbol{\varepsilon}^*\right] \\ &= \mathscr{E}\left[(\epsilon_z, 0, -\epsilon_x)\right. \\ &\quad \left. - \left(\frac{\beta\gamma}{\gamma+1}\right)(\epsilon_z\cos\omega_c t, \epsilon_z\sin\omega_c t, -\epsilon_x\cos\omega_c t)\right]\end{aligned}$$

so that

$$\left(\mathbf{B}' - \frac{\gamma}{\gamma+1}\boldsymbol{\beta}\times\mathbf{E}'\right)_{\pm} = \tfrac{1}{2}\mathscr{E}\cos\alpha\left(1 - \frac{\beta\gamma}{\gamma+1}e^{\pm i\omega_c t}\right).$$

Finally, then, (7.1.24) becomes

$$\frac{e\hbar\mathscr{E}\cos\alpha}{2\gamma mc}\left[\left(e^{i\omega_c t} - \frac{\beta\gamma}{\gamma+1}\right)\sigma_+ + \left(e^{-i\omega_c t} - \frac{\beta\gamma}{\gamma+1}\right)\sigma_-\right]. \tag{7.1.27}$$

This is the key result. It shows that the spin-raising and spin-lowering parts of the perturbing hamiltonian are different.

Now because, as mentioned, the radiation cone has opening angle $\approx 1/\gamma$, for our choice of $\mathbf{k}$ along OY the relevant times will be those for which $\boldsymbol{\beta}$ lies in such a cone, i.e. $|\omega_c t| \lesssim 1/\gamma$. Thus we can expand the exponentials in (7.1.27) and use the fact that $1-\beta$ is of order $1/\gamma^2$ for $\gamma \gg 1$, to obtain

$$\begin{aligned}H'_{\text{spin-flip}} &= \frac{e\hbar\mathscr{E}\cos\alpha}{2\gamma mc}\left\{\left(1 - i\omega_c t - \beta + \frac{\beta}{\gamma+1}\right)\sigma_+\right. \\ &\qquad \left. + \left(1 + i\omega_c t - \beta + \frac{\beta}{\gamma+1}\right)\sigma_-\right\} \\ &\simeq \frac{e\hbar\mathscr{E}\cos\alpha}{2\gamma^2 mc}\{(1-iu)\sigma_+ + (1+iu)\sigma_-\}\end{aligned} \tag{7.1.28}$$

where

$$u \equiv \gamma\omega_c t. \tag{7.1.29}$$

https://doi.org/10.1017/9781009402040.007 Published online by Cambridge University Press

Substituting for $\mathscr{E}$ from (7.1.14), the time integral in (7.1.20) is thus of the form

$$\frac{1}{i\hbar}\int \langle f|H'_{\text{spin-flip}}(t)|i\rangle dt = -\sqrt{\frac{2\pi\omega}{\hbar}}\frac{e\hbar\cos\alpha}{2\gamma^2 mc}\langle f|\sigma_{\pm}|i\rangle \times \int_{-1/\gamma_c}^{1/\gamma_c}(1\mp iu)e^{i[\omega t-\mathbf{k}\cdot\mathbf{R}(t)]}dt \quad (7.1.30)$$

where $\mathbf{R}(t)$ is the position vector along the trajectory.

The integrals are similar to those that occur in ordinary synchrotron radiation. They are approximated in a standard fashion, which we will not reproduce here. However, we shall at least show how the various powers of γ enter the transition rate. The exponent in (7.1.30), for our case of $\mathbf{k}$ along OY, and bearing in mind $|t|\lesssim(\gamma\omega_c)^{-1}$, is

$$\omega t - kR\sin\omega_c t = \omega\left(t-\frac{\beta}{\omega_c}\sin\omega_c t\right) = \omega\left(t-\beta t+\frac{\beta\omega_c^2 t^3}{6}+\cdots\right)$$
$$\cong \omega\left(\frac{t}{2\gamma^2}+\frac{\beta\omega_c^2 t^3}{6}+\cdots\right) \text{ for } \beta\simeq 1.$$

Both terms are of order $\omega_c^{-1}\gamma^{-3}$ whereas the terms left out are of order $\omega_c^{-1}\gamma^{-5}$.

The wave factor in (7.1.30) then becomes

$$\exp\left[i\frac{3}{2}\left(\frac{\omega}{\omega_{cr}}\right)u\left(1+\frac{u^2}{3}\right)\right] \quad (7.1.31)$$

where, conventionally,

$$\omega_{cr}\equiv 3\gamma^3\omega_c \quad (7.1.32)$$

is the characteristic frequency of synchrotron radiation. The integrals in (7.1.30) yield a result of the form

$$\frac{1}{\gamma\omega_c}\left[f_1\left(\frac{\omega}{\omega_{cr}}\right)\pm f_2\left(\frac{\omega}{\omega_{cr}}\right)\right]$$

where $f_{1,2}$ are in fact Bessel-type functions.

Gathering all factors from (7.1.14), (7.1.15) and (7.1.18) into (7.1.20), we have for the two spin-flip probabilities, per revolution,

$$\frac{dp^{\downarrow\uparrow/\uparrow\downarrow}}{d\Omega d\omega} = \frac{e^2\hbar\omega^3}{32\pi^2 m^2 c^5\gamma^6\omega_c^2}\left[f_1\left(\frac{\omega}{\omega_{cr}}\right)\pm f_2\left(\frac{\omega}{\omega_{cr}}\right)\right]^2. \quad (7.1.33)$$

We have cheated in (7.1.33) in not taking into account any angular dependence when $\mathbf{k}$ points outside the XY-plane. We account for this dependence roughly by taking $d\Omega\sim 2\pi/\gamma$. Then we divide by the period

https://doi.org/10.1017/9781009402040.007 Published online by Cambridge University Press

of revolution $2\pi/\omega_c$ to get a transition rate and integrate over ω, changing to the variable $\xi = \omega/\omega_{cr}$. The result is of the form

$$w^{\downarrow\uparrow/\uparrow\downarrow} \simeq \frac{e^2\hbar\omega_{cr}^4}{32\pi^2 m^2 c^5 \gamma^7 \omega_c}(a \pm b)$$

where $w^{\downarrow\uparrow}$ is the rate for the transition $\downarrow$ to $\uparrow$, $w^{\uparrow\downarrow}$ is the rate for the transition $\downarrow$ to $\uparrow$ and a, b are numbers of order unity. Substituting for ω_{cr} gives

$$w^{\downarrow\uparrow/\uparrow\downarrow} \approx \left(\frac{81}{32\pi^2}\right)\frac{e^2\hbar\gamma^5}{m^2c^2R^3}(a \pm b). \tag{7.1.34}$$

The precise numerical values of a and b depend upon a careful integration over angles and ω, but the essential kinematic dependence is correctly given by (7.1.34). An accurate treatment yields

$$w^{\uparrow\downarrow/\downarrow\uparrow} = \left(\frac{5\sqrt{3}}{16}\right)\frac{e^2\hbar\gamma^5}{m^2c^2R^3}\left(1 \pm \frac{8}{5\sqrt{3}}\right) \tag{7.1.35}$$

$$\equiv \frac{1}{2\tau_{ST}}\left(1 \pm \frac{8}{5\sqrt{3}}\right) \tag{7.1.36}$$

where τ_{ST}, as will be seen, is the characteristic rise time for the Sokolov–Ternov polarization to build up from an unpolarized state: one has

$$\tau_{ST} = \frac{8}{5\sqrt{3}}\frac{m^2c^2R^3}{e^2\hbar\gamma^5}. \tag{7.1.37}$$

For $R \sim 1000$ m, $\gamma \sim 10^5$, $\tau_{ST} \sim 5$ minutes. For LEP, running near the Z^0 mass, $\tau_{ST} \approx 310$ minutes.

Consider now the numbers of particles with spin up, $n_\uparrow(t)$, or down, $n_\downarrow(t)$, assuming that at time $t = 0$ $n_\uparrow = n_\downarrow$, i.e. the system is unpolarized. We have

$$\begin{aligned}\frac{dn_\uparrow}{dt} &= w^{\uparrow\downarrow}n_\downarrow - w^{\downarrow\uparrow}n_\uparrow = nw^{\uparrow\downarrow} - n_\uparrow w \\ \frac{dn_\downarrow}{dt} &= w^{\downarrow\uparrow}n_\uparrow - w^{\uparrow\downarrow}n_\downarrow = nw^{\downarrow\uparrow} - n_\downarrow w\end{aligned} \tag{7.1.38}$$

where

$$w \equiv w^{\uparrow\downarrow} + w^{\downarrow\uparrow} = 1/\tau_{ST} \tag{7.1.39}$$

and

$$n = n_\uparrow + n_\downarrow = \text{ constant.}$$

The degree of polarization along OZ is

$$\mathscr{P}(t) = \frac{n_\uparrow(t) - n_\downarrow(t)}{n}. \tag{7.1.40}$$

https://doi.org/10.1017/9781009402040.007 Published online by Cambridge University Press

So

$$\frac{d\mathscr{P}}{dt} = \frac{1}{n}\left(\frac{dn_\uparrow}{dt} - \frac{dn_\downarrow}{dt}\right) = \left(w^{\uparrow\downarrow} - w^{\downarrow\uparrow}\right) - w\mathscr{P}.$$

Thus

$$\mathscr{P}(t) = \frac{w^{\uparrow\downarrow} - w^{\downarrow\uparrow}}{w}\left(1 - e^{-t/\tau_{ST}}\right) \tag{7.1.41}$$

The ultimate polarization, in a perfect machine, due to the Sokolov–Ternov mechanism is thus

$$\mathscr{P}_{ST} = \frac{8}{5\sqrt{3}}. \tag{7.1.42}$$

It seems clear that the precise value of $\mathscr{P}_{ST}$ is *not* related to some simple physical fact. It emerges from integrals over Bessel functions. Moreover, Jackson (1976) studied the situation for arbitrary values of g, and for a certain range of *positive* g-values, $0 < g < 1.2$, finds that $\mathscr{P}_{ST}$ even has the opposite sign to (7.1.42)!

7.1.1 Imperfect storage rings

In the previous section we dealt with a perfect storage ring, i.e. one that is absolutely planar with its guide field perpendicular to the orbit plane and with no magnetic imperfections.

In that case there is a unit vector **n**, along or opposite to the guide field, such that a mean spin vector initially along **n** will remain so, independent of the azimuthal angle θ that specifies the position of the particle on its orbit. A general spin vector, not along **n**, will precess around **n** as the particle moves in its orbit.

In the case of an imperfect machine there is no such fixed direction, but for a particle on a closed orbit there does exist a direction $\mathbf{n}(\theta)$, varying with the particle position, which is periodic, i.e.

$$\mathbf{n}(\theta + 2\pi) = \mathbf{n}(\theta) \tag{7.1.43}$$

and such that if the mean spin vector $\mathbf{s}(\theta)$ is initially along $\mathbf{n}(\theta)$ at some angle θ it will continue to point along $\mathbf{n}(\theta)$ as θ changes. Thus $\mathbf{n}(\theta)$ represents a periodic solution to the equations of spin motion (6.3.23).

For a closed orbit the magnetic fields experienced by the particle are periodic i.e. $\mathbf{B}(\theta + 2\pi) = \mathbf{B}(\theta)$, from which it is easy to show that any solution to the equation of spin motion must satisfy

$$\mathbf{s}(\theta + 2\pi) = R_\theta \mathbf{s}(\theta) \tag{7.1.44}$$

where R_θ is some rotation, which depends on θ and is itself periodic, $R_{\theta+2\pi} = R_\theta$.

https://doi.org/10.1017/9781009402040.007 Published online by Cambridge University Press

If, now, we resolve an arbitrary $\mathbf{s}(\theta)$ into components along $\mathbf{n}(\theta)$ and orthogonal to it, then (7.1.43) and (7.1.44) clearly imply that the components of $\mathbf{s}(\theta)$ orthogonal to $\mathbf{n}(\theta)$ rotate around $\mathbf{n}(\theta)$ by a fixed number of radians per revolution. Moreover, since eqns (6.3.23)–(6.3.27) hold for an arbitrary field $\mathbf{B}$, the angle involved is simply $2\pi\nu_s$ where ν_s is the spin tune; $\nu_s = G\gamma$, introduced in (6.3.27). In short, in an imperfect machine the mean spin vector precesses about a periodic solution $\mathbf{n}(\theta)$ instead of about the unique guide field in a perfect machine. To the extent that one is only dealing with very small imperfections and there are no special spin rotator magnets in the ring, $\mathbf{n}(\theta)$ should deviate only slightly from the guide field direction except in the vicinity of the spin resonances discussed in subsection 6.3.2.

The mechanism of the natural Sokolov–Ternov polarization discussed in Section 7.1 continues to operate in the case of non-uniform fields but the direction of the equilibrium polarization is along $\mathbf{n}(\theta)$ rather than the guide field. The problem of imperfection and intrinsic resonances, which bedevils the acceleration of polarized protons (where the growing energy implies a growing spin tune which thus continually intercepts resonance values) ought not, ideally, to affect a storage ring, where the particles are circulating at a fixed energy chosen so that ν_s is well clear of a resonance value. In reality however, there may be a significant spread of energies so that electrons far from the central value may hit a depolarizing resonance.

The main mechanism for the spread in energies is discrete photon emission in addition to the usual classical synchrotron radiation. It is important for electrons, but totally negligible for protons. And, as we now explain, it gives rise to an important depolarizing effect. The probabilities for spin-flip in the emission of the photon ($w^{\uparrow\downarrow}$ and $w^{\downarrow\uparrow}$ given in (7.1.34)) are orders of magnitude smaller than the non-flip probabilities, so the emission may be considered to take place without spin-flip.

Photon emission is a random process, the time scale for which is minute in comparison with changes in orbit position or direction of the mean spin vector. The only significant effect on an electron following a closed orbit is thus its energy loss, so that it finds itself with too little energy to remain on its original orbit. It thus begins to execute horizontal betatron oscillations, and these lead to vertical oscillations as well.

Some indication of the mechanisms at work can be elicited by supposing that the electron was originally on the central closed orbit at an energy well clear of depolarizing resonances, with its mean spin vector along the associated periodic solution $\mathbf{n}_0(\theta)$. After emission it is on an orbit for which $\mathbf{n}(\theta) \neq \mathbf{n}_0(\theta)$, so its spin vector begins to precess about $\mathbf{n}(\theta)$. As the electron gradually picks up RF energy its orbit oscillations are damped out, its orbit approaches the central orbit and $\mathbf{n}(\theta) \to \mathbf{n}_0(\theta)$. In this relatively slow process the mean spin vector continues to precess

about $\mathbf{n}(\theta)$, adiabatically following its change until it ends up precessing about $\mathbf{n}_0(\theta)$. Since it was originally *along* $\mathbf{n}_0(\theta)$ its component along $\mathbf{n}_0(\theta)$ has decreased.

In fact each electron emits many photons and, since the emissions are uncorrelated both in time and energy, the perturbations give rise to a random walk of the mean spin vector superposed on any coherent precession motion. The stochastic nature of the photon emission results in a diffusion of the spin vectors and hence to a depolarization of the beam.

Bearing in mind that only a tiny fraction of emissions involve spin-flip and thus contribute to the Sokolov–Ternov mechanism, it is clear that the spin diffusion is potentially a very strong effect and the achievable polarization $\mathscr{P}_{\max}$ may be much less than $\mathscr{P}_{\mathrm{ST}}$.

The strength of the depolarizing process can be characterized by a diffusion time τ_{D}. The competition between the Sokolov–Ternov and diffusion mechanisms then results in an asymptotic maximal polarization

$$\mathscr{P}_{\max} = \left(\frac{\tau_{\mathrm{D}}}{\tau_{\mathrm{ST}} + \tau_{\mathrm{D}}}\right) \mathscr{P}_{\mathrm{ST}}. \tag{7.1.45}$$

The polarization build-up time is reduced to

$$\tau = \left(\frac{\mathscr{P}_{\max}}{\mathscr{P}_{\mathrm{ST}}}\right) \tau_{\mathrm{ST}}. \tag{7.1.46}$$

Without special precautions, τ_{D} can be quite small compared with τ_{ST}, leading to a serious loss of beam polarization. It is thus essential to take steps to counteract the depolarizing mechanism.

The horizontal and vertical orbit oscillations are not purely simple harmonic. However, they may be expanded in a Fourier series with frequencies per revolution specified by integers k. The actual associated integer depolarization resonances then occur at $\nu_{\mathrm{s}} = k$, but even for $\nu_{\mathrm{s}} \neq k$ they have an influence that depends upon their strength and their proximity to ν_{s}.

The vertical orbit oscillations are the most damaging for the polarization since the result is that the spin-vector is rotated away from the essentially vertical direction $\mathbf{n}_0(\theta)$. It is possible to compensate for these by the method of *harmonic spin matching* (Rossmanith and Schmidt, 1985; Barber *et al.*, 1994). Additional vertical distortions ('bumps') are introduced at strategic positions along the orbit and tuned to correspond to those harmonic components of the vertical oscillations closest to the spin tune.

Initially such corrections were implemented empirically by varying the bump amplitudes and monitoring the resultant polarization. With improved accuracy in monitoring the beam position and a suitable feedback system the optimal corrections can be applied automatically.

These techniques have been used with great success at LEP at CERN and at PETRA and HERA in Hamburg. A detailed discussion of the

approach used at HERA can be found in Barber (1994). A general summary of the state of the art in this field is given in Barber (1996).

7.2 Polarization at LEP and HERA

Ever since the mid-1980s there have been studies of the possibility of having polarized e^+e^- beams in LEP, this *transverse* polarization arising from the Sokolov–Ternov effect discussed in Section 7.1. These studies were catalysed by the realization that experiments with *longitudinally* polarized leptons would allow very accurate measurements of the parameters of the Standard Model of electroweak interactions, as will be discussed in Chapter 9. It was envisaged that the transverse polarization would be rotated into the longitudinal direction by special magnets without difficulty.

But there were major problems and doubts. The near-miraculous natural polarization $\mathscr{P}_{ST} \approx 92\%$ derived in Section 7.1 assumes a perfect machine. All the difficulties that beset the acceleration of polarized protons (subsection 6.3.2) in an imperfect machine apply to electrons as well; in addition, the greater synchrotron radiation leads to bigger problems with synchrotron oscillations.

Nonetheless an extraordinary collaboration of accelerator and particle physicists at CERN and HERA has succeeded in mastering many of the difficulties.

7.2.1 Polarization at LEP

An early attempt to calculate theoretically the expected behaviour of the polarization as a function of beam energy is shown in Fig. 7.1 (Koutchouk and Limberg, 1988). The first observation of a stable transverse polarization of $(9.1 \pm 0.3 \pm 1.8)\%$ at LEP was reported in 1991 (Knudsen *et al.*, 1991) and despite its smallness soon led to an improvement in our knowledge of the parameters of the Standard Model, albeit in an indirect way – by an improved calibration of the beam energy in LEP and thereby of the mass and width of the Z^0.

The idea is to use *resonant depolarization.* A frequency-controlled radial rf magnetic field causes the spin vector of the particle to precess away from its transverse (vertical) direction. An artificial depolarizing resonance occurs when the frequency ν_{dep} of the oscillatory magnetic field equals the spin precession frequency, i.e. when (see eqn (6.3.27))

$$\nu_{dep} = \nu_{dep}^{res} \equiv G\gamma f_{rev} = \frac{GE}{m_e c^2} f_{rev} \tag{7.2.1}$$

https://doi.org/10.1017/9781009402040.007 Published online by Cambridge University Press

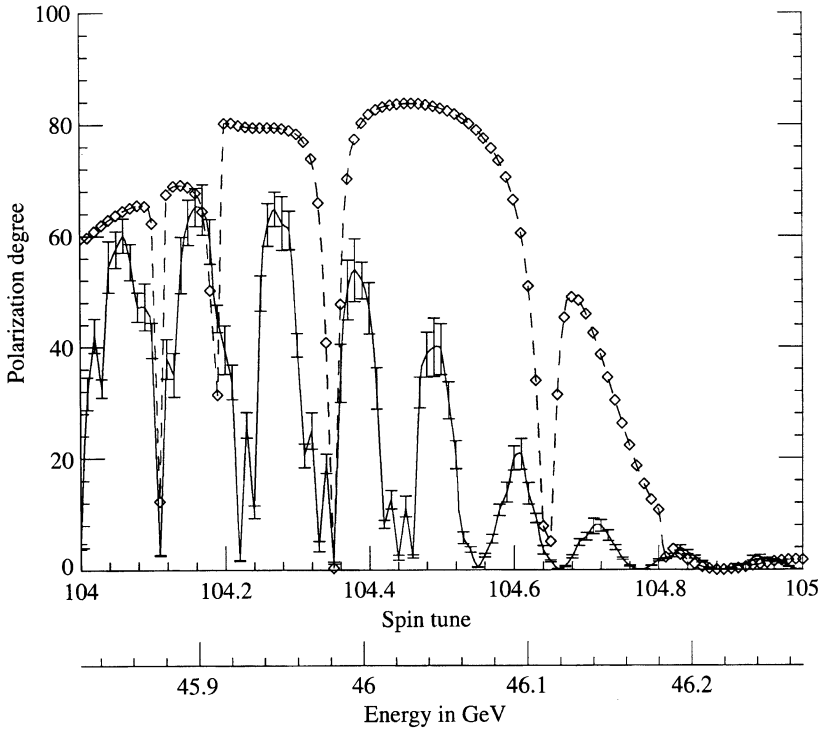

Fig. 7.1 Early theoretical estimate, in two models, of the beam polarization as a function of beam energy at LEP (courtesy of J.P. Koutchouk): diamonds on broken line, linear calculation; solid line with error bars, spin tracking.

where f_{rev} is the particle's frequency of revolution at energy E and, for electrons, G is known to fantastic accuracy:

$$G = \frac{g}{2} - 1 = 1.159652188 \times 10^{-3}. \tag{7.2.2}$$

The spin tune $\nu_s \equiv G\gamma$ can be written as

$$\nu_s = N_s + \delta\nu_s, \tag{7.2.3}$$

where N_s is an integer ($N_s = 103$ at the Z^0 mass), and it is then sufficient to measure $\delta\nu_{\text{dep}}^{\text{res}} \equiv \delta\nu_s f_{\text{rev}}$ at resonance. One ends up with a formula for the beam energy,

$$E_{\text{beam}} = 0.4406486 \left(N_s + \frac{\delta\nu_{\text{dep}}^{\text{res}}}{f_{\text{res}}} \right) \text{GeV}, \tag{7.2.4}$$

that led, in 1991, to a LEP beam energy calibration to an accuracy of $\lesssim$1 MeV i.e. about one part in 10^5!

https://doi.org/10.1017/9781009402040.007 Published online by Cambridge University Press

In fact this method had already been used with great success in lower-energy electron machines, VEPP2 and VEPP4 at Novosibirsk, DORIS in Hamburg and CESR at Cornell, leading to greatly improved precision in the measurements of the masses of the vector mesons $\omega, \phi, J/\psi, \psi'$, and the upsilon family Υ, Υ' and Υ'.

In a perfect LEP machine the rise time τ_{ST} to reach the polarization $\mathscr{P}_{ST} = 92\%$ is found from (7.1.37) to be about 5 hours at the Z^0 mass, an enormously long time during which, in an imperfect machine, all kinds of depolarizing effects will operate. The situation, as explained earlier, can be summarized by introducing a characteristic depolarization time τ_D, in which case the asymptotic polarization is reduced to

$$\mathscr{P}_\infty = \frac{1}{1 + \tau_{ST}/\tau_D} \mathscr{P}_{ST} \tag{7.2.5}$$

and, in parallel, the rise time is reduced to

$$\tau = \frac{1}{1 + \tau_{ST}/\tau_D} \tau_{ST}. \tag{7.2.6}$$

The original polarization of about 9% at LEP has been steadily improved upon, using the method of harmonic spin matching. In this way polarizations of about 60% have been achieved for non-interacting beams.

Another problem stems from the solenoids used by the experimental groups at LEP, which have strong longitudinal fields that cause the mean spin vector to rotate about a longitudinal axis. This has been solved by introducing additional bumps before and after each solenoid to compensate for the longitudinal rotation.

More recently studies have begun of the effect of interactions on the polarization. It has been possible to attain a stable transverse polarization of about 40% with one interaction region and with a high luminosity of about 1.5×10^{30} cm^{-2} s^{-1} (Assmann *et al.*, 1995), but no comprehensive spin physics programme was undertaken.

Given that extremely precise measurements of the electroweak parameters are envisaged, it is important to try to eliminate sources of systematic error, principally in the measurements of the polarization of the beams and in the normalization of data samples taken with different settings of the e^+e^- helicities. A very clever trick (Blondel, 1998; Placidi and Rossmanith, 1985) permits the elimination of both these errors. The transverse polarization of the e^+ and e^- will be in opposite directions and after rotation to the longitudinal direction this will still be true. Thus the (longitudinal) spins of e^+ and e^- will be opposite, so that the *helicities* of the e^+ and e^- will be the same. It is relatively easy to depolarize a beam.

https://doi.org/10.1017/9781009402040.007 Published online by Cambridge University Press

Moreover, this can be done to the individual bunches in the beam, so that one can have a pattern of bunch–bunch collisions with various settings of the spins, as shown in Fig. 7.2. For the four types of collision indicated, the total cross-sections depend upon the degree of longitudinal polarization $\mathscr{P}_e$, $\mathscr{P}_{\bar{e}}$ of the electron and positron beams and upon an *asymmetry parameter* A_{LR}. As explained in Chapter 9, an accurate measurement of A_{LR} sheds valuable light on the electroweak parameters. One has

$$\begin{aligned}\sigma_1 &= \sigma(1 + \mathscr{P}_{\bar{e}} A_{\mathrm{LR}}) \\ \sigma_2 &= \sigma(1 - \mathscr{P}_e A_{\mathrm{LR}}) \\ \sigma_3 &= \sigma \\ \sigma_4 &= \sigma\,[1 - \mathscr{P}_e \mathscr{P}_{\bar{e}} + (\mathscr{P}_{\bar{e}} - \mathscr{P}_e) A_{\mathrm{LR}}]\end{aligned} \tag{7.2.7}$$

where σ is the unpolarized cross-section.

Remarkably, these four measurements permit us to deduce the values of $\mathscr{P}_e$, $\mathscr{P}_{\bar{e}}$ and A_{LR}! It should be noted that this is a fairly miraculous situation. It happens only because in the Standard Model we are able to show that the coefficient of $\mathscr{P}_{\bar{e}}\mathscr{P}_e$ is -1.

7.2.2 Polarization at HERA

Ever since its conception there have been plans to polarize the leptons in the $e^{\pm}$–proton collider HERA, one objective being the study of polarized deep inelastic lepton–proton scattering by the HERMES collaboration utilizing a polarized-proton gas cell (see subsection 6.2.2) as target. The project gained much impetus from the startling results of the 1988 European Muon Collaboration experiment involving longitudinally polarized muons colliding with a polarized proton target (this is discussed in Chapter 11).

The HERMES collaboration began its first data-taking in 1995. Consideration is now being given to the possibility of polarizing the 820

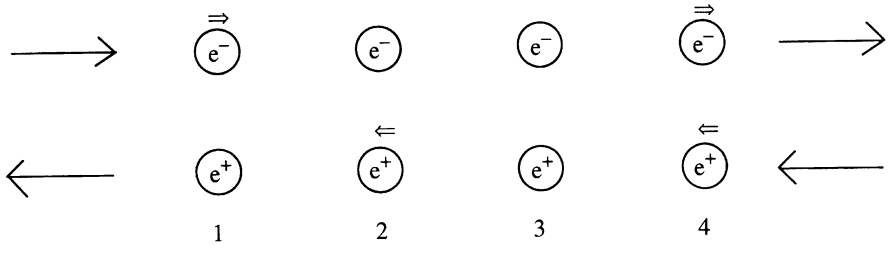

Fig. 7.2 A possible setting of the spins in successive e^+ and e^- bunches at LEP: the number 1–4 show four kinds of collision. Absence of an arrow $\Rightarrow$ indicates an unpolarized bunch.

https://doi.org/10.1017/9781009402040.007 Published online by Cambridge University Press

GeV proton beam as well. Such a facility would allow very interesting experiments on the polarized structure function $g_1(x, Q^2)$ at very small x and large Q^2 and also could provide much needed information about the polarization of gluons in polarized protons (see Section 11.6).

Unlike LEP the natural rise time for the transverse Sokolov–Ternov polarization, assuming a perfect machine, is quite short: for $e^{\pm}$ 40 minutes at 27 GeV and 11 minutes at 35 GeV. When the machine was optimized for polarization using empirical harmonic orbit corrections, as discussed in subsection 7.1.1, the depolarization time τ_D could be made as long as 2 hours. Consequently, stable transverse polarizations of electrons or positrons of 60–70% were achieved routinely during 1995, well above the 50% design goal of the HERMES experiment.

In May 1994 the spin rotators were brought into operation and HERA became the first high energy electron machine to achieve *longitudinal* polarization. The so called 'Mini-rotators' (Buon and Steffen, 1986) consist of a sequence of dipole magnets designed to deflect the beam sequentially in the vertical and horizontal directions, as shown in Fig. 7.3. At each small angular deflection of the beam the component of the mean spin vector perpendicular to the field of the bending magnet precesses through an angle which is $1 + G\gamma = 63.5$ times bigger than the deflection angle; see (6.3.27).

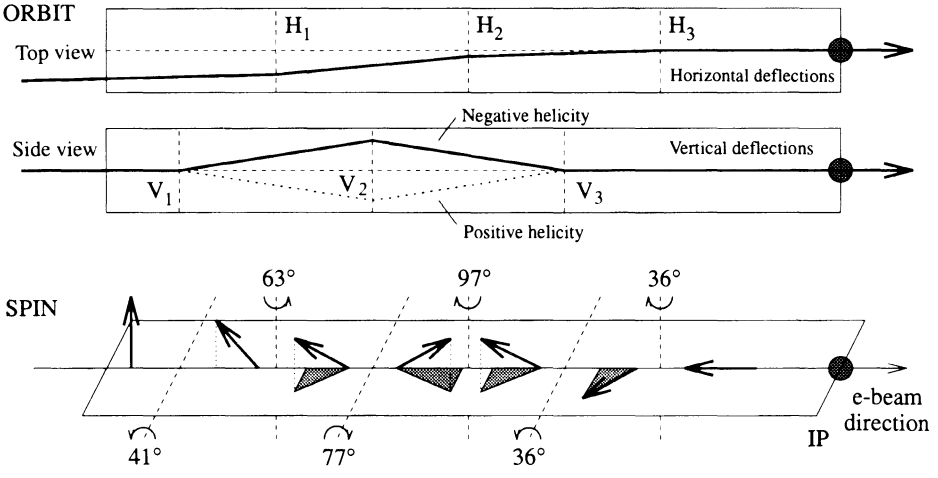

Fig. 7.3 Schematic diagram of a 'mini-rotator', showing horizontal and vertical beam deflections at the points $H_{1,2,3}$ and $V_{1,2,3}$ and the corresponding precession of the spin vector (courtesy of M. Düren).

https://doi.org/10.1017/9781009402040.007 Published online by Cambridge University Press

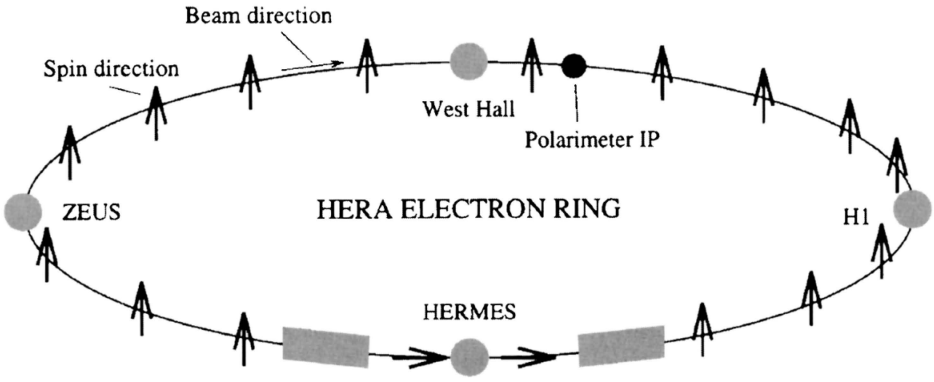

Fig. 7.4 Layout at the HERA ring showing the spin rotators and an idealized picture of the mean spin directions (courtesy of M. Düren).

Of course, once past the HERMES experimental region the longitudinal polarization must be rotated back to the transverse direction. The layout of rotators, spin directions etc. around the HERA ring is shown in Fig. 7.4.

The system has worked outstandingly well and stable longitudinal polarizations of about 70% are routinely achieved. An exciting and challenging investigation of the spin structure of the nucleon is in full swing and many interesting results have already emerged.

7.3 Polarization at SLC

In the Stanford linear collider the acceleration of the $e^{\pm}$ beams takes place along straight sections of the accelerator, so there is no Sokolov–Ternov effect in operation and the polarization must be produced at the electron source. The $e^{\pm}$ beams are brought together for collision along circular arms of the accelerator, but, since they only transverse these arcs once, there is no danger of resonant build-up of the depolarization effects that plague circular accelerators.

The principal challenge, then, is to produce a source of polarized electrons with a stable high degree of polarization and with a high output intensity. There is a long history of attempts to construct these sources. In more recent times, the desire to study the spin structure of the proton at SLAC in the 1970s led to the development of a photoionization source that played an essential rôle in the first experiments on the seminal process of polarized deep inelastic scattering (Chapter 11). However,

https://doi.org/10.1017/9781009402040.007 Published online by Cambridge University Press

the need for the much higher current required for the SLC led to the development of a new polarized source based upon photoemission from gallium arsenide (GaAs). The use of molecular beam epitaxy to grow thin layers of strained GaAs on wafers of bulk GaAs led ultimately to the achievement of polarizations above 80% with short bunch currents of a few amperes. The electrons are photoexcited by a pulsed, tunable laser. A comprehensive description of the SLAC polarized electron source, shown in Fig. 7.5, can be found in the review article by Alley *et al.* (1995).

The physical mechanism responsible for the polarization of the photoelectrons can be understood from the energy level diagrams (Fig. 7.6) for ordinary GaAs (top figure) and strained GaAs (lower figure). The solid and broken lines correspond respectively to transitions induced by right circularly polarized light (σ^+), and left circularly polarized light (σ^-). E_g is the band gap. The numbers in circles are the relative transition probabilities for the transitions.

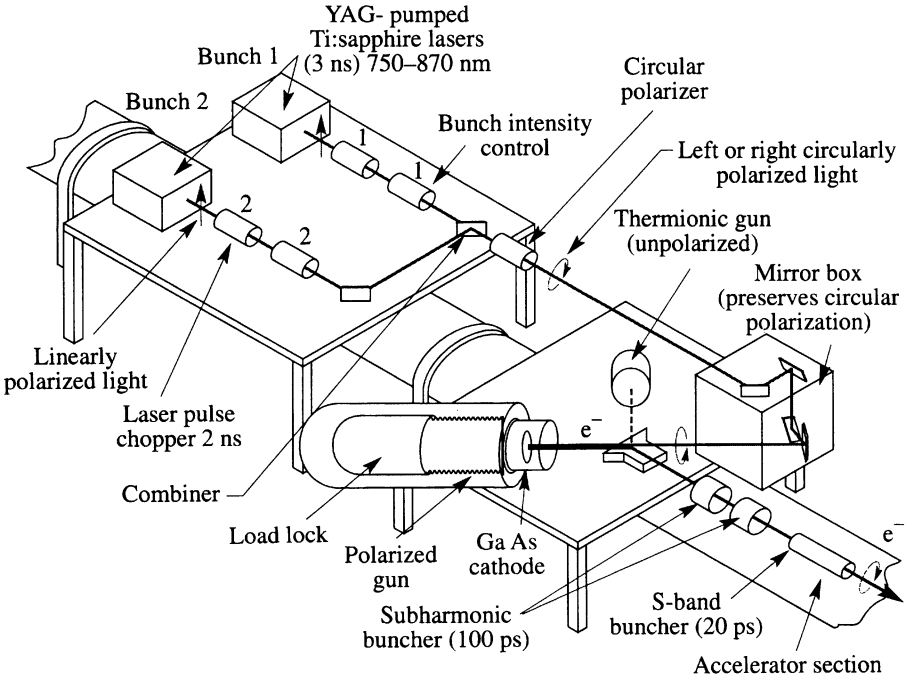

Fig. 7.5 The Stanford linear accelerator polarized electron source (courtesy of J. Clendenin and L. Piemontese).

https://doi.org/10.1017/9781009402040.007 Published online by Cambridge University Press

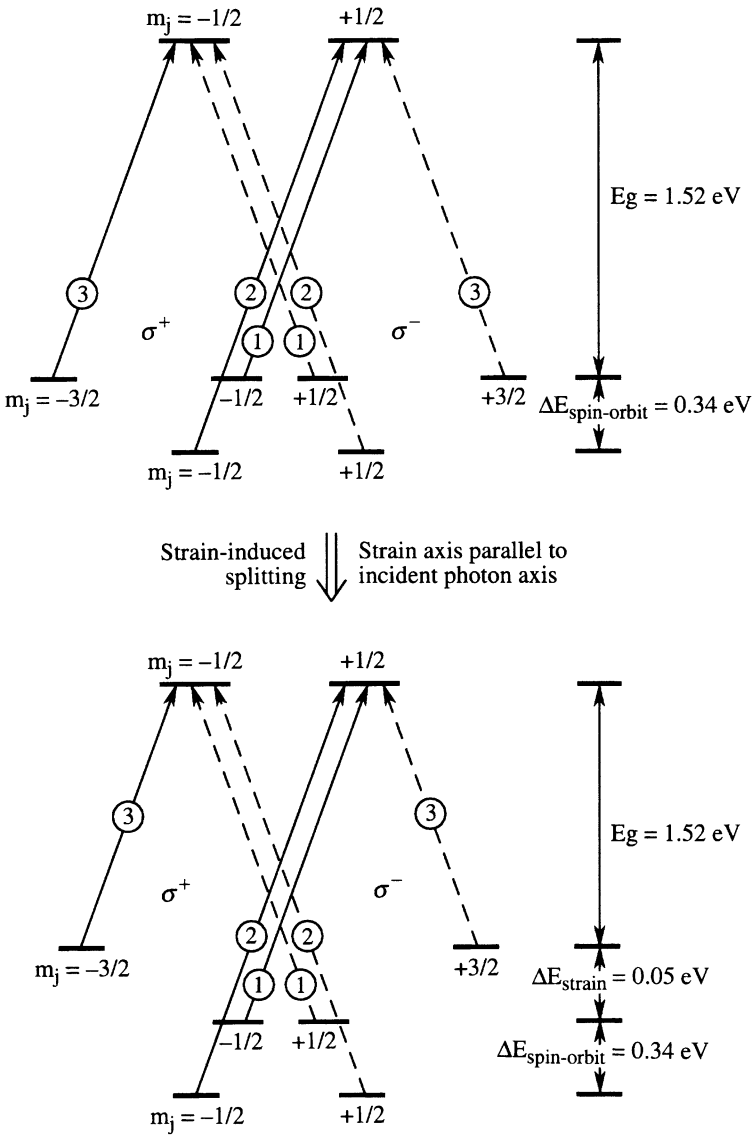

Fig. 7.6 Energy level diagram for ordinary GaAs (upper figure) and strained GaAs (lower figure) (courtesy of J. Clendenin and L. Piemontese).

Let us concentrate on the case of left circularly polarized light. In the unstrained case, if the light frequency is adjusted so that

$$E_g < h\nu < E_g + \Delta E_{\text{spin-orbit}}$$

then the only transitions into the conduction band are $m_j = 1/2 \rightarrow m_j = -1/2$, with relative transition rate 1, and $m_j = 3/2 \rightarrow m_j = 1/2$, with

https://doi.org/10.1017/9781009402040.007 Published online by Cambridge University Press

relative transition rate 3. The polarization is then

$$\mathscr{P}_{\sigma^-} = \frac{N(m_j = 1/2) - N(m_j = -1/2)}{N(m_j = 1/2) + N(m_j = -1/2)} = \frac{1}{2} \tag{7.3.1}$$

with a similar argument giving $\mathscr{P}_{\sigma^+} = -1/2$.

In the strained case the degenerate valence band levels are split. Thus by choosing the light frequency such that

$$E_g < h\nu < E_g + \Delta E_{\text{strain}}$$

one can eliminate the transition $m_j = 1/2 \rightarrow m_j = -1/2$, leaving only the transition to the $m_j = 1/2$ state. This yields, in principle, 100% positive polarization, $\mathscr{P}_{\sigma^-} = 1$, and similarly for right circularly polarized light, $\mathscr{P}_{\sigma^+} = -1$.

The SLAC polarized electron source has functioned extremely efficiently. It has played an important rôle in testing the Standard Model of electroweak interaction via e^+e^- collisions in the SLC (Chapter 9) and is, at present, providing data of extraordinary accuracy in polarized deep inelastic scattering, where the polarized electron beam collides with polarized fixed targets of hydrogen, deuterium and helium-3 (Chapter 11).